Brain Structure and Function (2019) 224:2213–2230
https://doi.org/10.1007/s00429-019-01898-6

ORIGINAL ARTICLE

Deficiency of the palmitoyl acyltransferase ZDHHC7 impacts brain and behavior of mice in a sex-specific manner

Christa Hohoff[1] · Mingyue Zhang[1] · Oliver Ambrée[1,2] · Mykola Kravchenko[1] · Jens Buschert[1,3] · Nicole Kerkenberg[1,3] · Nataliya Gorinski[4] · Dalia Abdel Galil[4] · Christiane Schettler[1] · Kari Lavinia vom Werth[1] · Maximilian F.-J. Wewer[1] · Ilona Schneider[1,3] · Dominik Grotegerd[1] · Lydia Wachsmuth[5] · Cornelius Faber[5] · Boris V. Skryabin[6,7] · Juergen Brosius[7,8] · Evgeni Ponimaskin[4] · Weiqi Zhang[1]

Received: 12 April 2019 / Accepted: 31 May 2019 / Published online: 10 June 2019

Abstract

The palmitoyl acyltransferase ZDHHC7 belongs to the DHHC family responsible for the covalent attachment of palmitic acid (palmitoylation) to target proteins. Among synaptic proteins, its main targets are sex steroid receptors such as the estrogen receptors. When palmitoylated, these couple to membrane microdomains and elicit non-genomic rapid responses. Such coupling is found particularly in cortico-limbic brain areas which impact structure, function, and behavioral outcomes. Thus far, the functional role of ZDHHC7 has not been investigated in this context. To directly analyze an impact of ZDHHC7 on brain anatomy, microstructure, connectivity, function, and behavior, we generated a mutant mouse in which the *Zdhhc7* gene is constitutively inactivated. Male and female *Zdhhc7*$^{-/-}$ mice were phenotypically compared with wild-type mice using behavioral tests, electrophysiology, protein analyses, and neuroimaging with diffusion tensor-based fiber tractography. *Zdhhc7*-deficiency impaired excitatory transmission, synaptic plasticity at hippocampal Schaffer collateral CA1 synapses, and hippocampal structural connectivity in both sexes in similar manners. Effects on both sexes but in different manners appeared in medial prefrontal cortical synaptic transmission and in hippocampal microstructures. Finally, *Zdhhc7*-deficiency affected anxiety-related behaviors exclusively in females. Our data demonstrated the importance of *Zdhhc7* for assembling proper brain structure, function, and behavior on a system level in mice in a sex-related manner. Given the prominent role of sex-specificity also in humans and associated mental disorders, *Zdhhc7*$^{-/-}$ mice might provide a promising model for in-depth investigation of potentially underlying sex-specifically altered mechanisms.

Keywords Palmitoylation · *Zdhhc7*-deficiency · Constitutive knockout mouse · Small animal imaging · Electrophysiological recordings · Behavioral phenotyping

Introduction

S-palmitoylation is a post-translational covalent attachment of 16-C fatty acid palmitate to cysteine residue(s) via formation of a thioester bond (Linder and Deschenes 2007). This reversible modification increases protein hydrophobicity and thereby changes membrane attachment and interactions with lipid bilayers, protein sorting, and functions (Fukata and Fukata 2010; Shipston 2011). Palmitoylation is highly abundant in neurons, where it regulates protein trafficking to membrane microdomains, and its alteration is involved in different brain-derived disorders (Antinone et al. 2013; Butland et al. 2014; Fukata and Fukata 2010; Mitchell et al. 2014). S-palmitoylation is primarily catalyzed by palmitoyl acyltransferases (PATs) based on a conserved

Christa Hohoff, Mingyue Zhang, and Oliver Ambrée authors contributed equally to this work.

Electronic supplementary material The online version of this article (https://doi.org/10.1007/s00429-019-01898-6) contains supplementary material, which is available to authorized users.

✉ Christa Hohoff
hohoffch@uni-muenster.de

✉ Weiqi Zhang
wzhang@uni-muenster.de

Extended author information available on the last page of the article

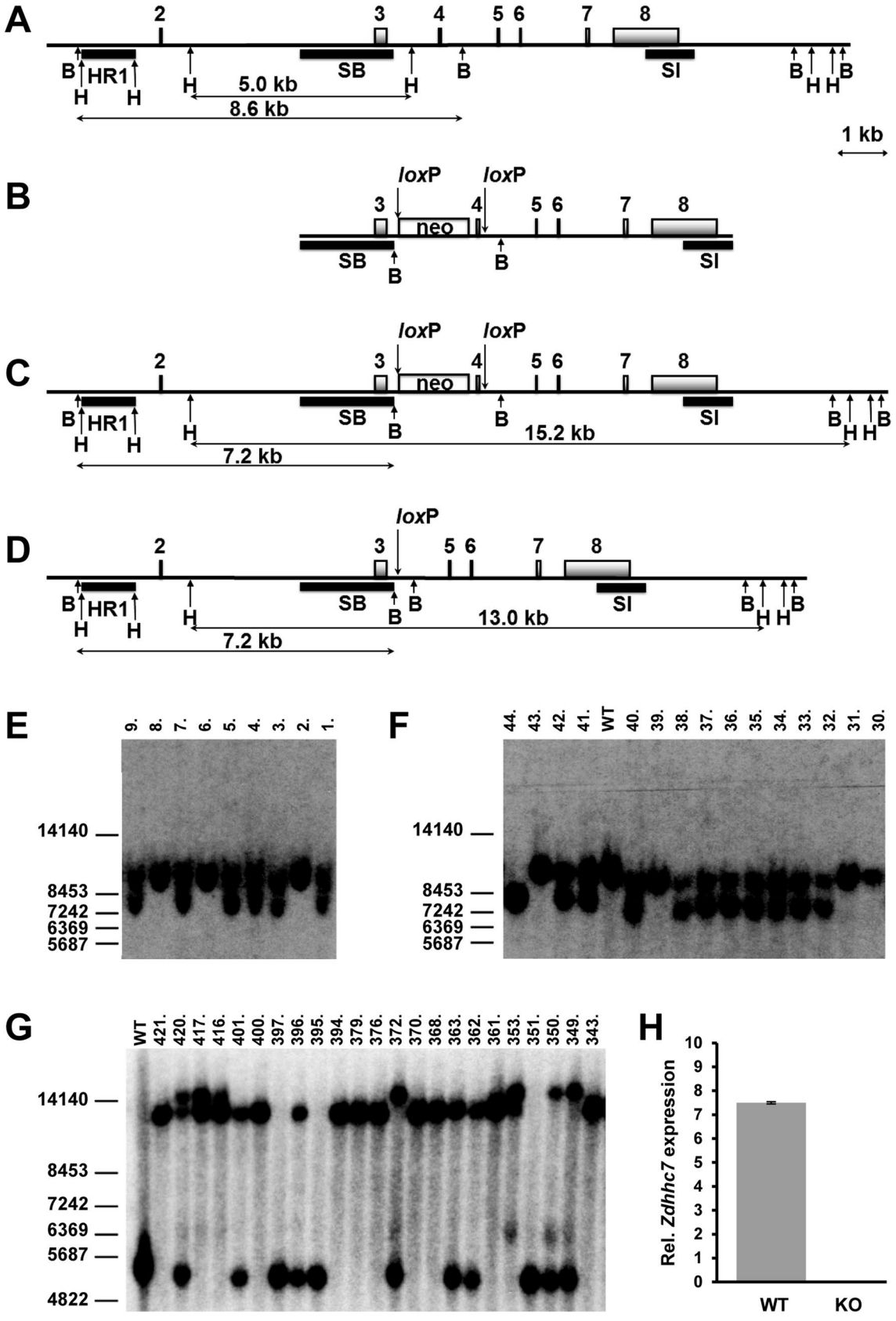
A
2
3
4
5 6
7
8
B
HR1
H
H
H
5.0 kb
SB
H
B
SI
B
H H
B
8.6 kb
1 kb
B
loxP
loxP
3
4
5 6
7
8
neo
SB
B
B
SI
C
loxP
loxP
2
3
4
5 6
7
8
neo
B
HR1
H
H
H
SB
B
B
SI
B
H H
B
7.2 kb
15.2 kb
D
loxP
2
3
5 6
7
8
B
HR1
H
H
H
SB
B
B
SI
B
H H
B
7.2 kb
13.0 kb
E
9. 8. 7. 6. 5. 4. 3. 2. 1.
14140
8453
7242
6369
5687
F
44. 43. 42. 41. WT 40. 39. 38. 37. 36. 35. 34. 33. 32. 31. 30.
14140
8453
7242
6369
5687
G
WT 421. 420. 417. 416. 401. 400. 397. 396. 395. 394. 379. 376. 372. 370. 368. 363. 362. 361. 353. 351. 350. 349. 343.
14140
8453
7242
6369
5687
4822
H
Rel. Zdhhc7 expression
10
9
8
7
6
5
4
3
2
1
0
WT
KO

◂**Fig. 1** Generation of *Zdhhc7*$^{-/-}$ mice. The upper section depicts the mouse *Zdhhc7* gene around target exon 4 during steps **a–d**. **a** Wild-type locus with intronic/intergenic regions (indicated as line), exons (gray filled boxes with numbers above the line), restriction endonuclease sites *Bam*HI (B) and *Hin*dIII (H) (arrows below), and restriction fragments (in kb; horizontal arrows). Sequences used as probes for Southern blots are shown as HR1, SB, and SI (black filled boxes below the line). **b** Targeting vector structure (without negative selection marker and plasmid backbone) with *lox*P sites (arrows above) and neomycin-resistance cassette [neo; empty box flanked by two FRT sites (not shown)]. **c** Locus after homologous recombination with neo cassette (present in intron 3) and target exon 4, flanked by *lox*P sites. **d** Genomic locus after CRE-mediated exon 4 deletion. The lower parts **e–g** illustrate corresponding parts of Southern blot analysis of genomic DNA (from mouse tail biopsies; positions of size markers in bp on the left; for complete blots see Online Resource). **e** Southern blot analysis (HR1 after *Bam*HI restriction digestion) validated correctly targeted *Zdhhc7*$^{+/-}$ alleles (WT: 8.6 kb, targeted allele: 7.2 kb) in F1 offspring ($^{+/-}$ in lanes 1, 3–5, 7, 9). (**f**) Southern blot analysis as in e) in F2 offspring ($^{+/-}$ in lanes 32–38, 40, 41, 42; $^{-/-}$ in 44; $^{+/+}$ in WT, 30, 31, 43). **g** CRE-mediated exon 4 deletion validated by Southern blot (SB after *Hin*dIII digestion; WT: 5.0 kb, targeted allele: 15.2 kb, deleted allele: 13.0 kb). Genotype $^{+/-}$ is found in lanes 362, 363, 396, 401, and genotype $^{-/-}$ in lanes 343, 361, 368, 370, 376, 379, 394, 400, and 421. Samples 353, 416, and 417 are heterozygous for the targeted allele and exon 4 deletion. Sample 420 contains all three alleles and possibly was derived from mosaic mice due to incomplete CRE-mediated exon 4 deletion. The lower right part (**h**) illustrates qPCR analysis of *Zdhhc7* mRNA (from mouse mPFC tissue; WT: $n=7$, KO: $n=7$). TaqMan gene expression assay spanning exons 4–5 validated deletion of target exon 4 (essential for catalytic DHHC domain) by loss of *Zdhh7* expression in *Zdhhc7*$^{-/-}$ (KO) mice compared to consistent *Zdhh7* expression in wild-type (WT) mice (expression relative to endogenous control gene *Gapdh*)

Asp–His–His–Cys (DHHC) domain essential for PAT activity (Lemonidis et al. 2015). Humans as well as mice harbor 23 PATs, which contain a conserved zinc finger domain (ZDHHC) and are involved in neuronal development, synaptic function, and plasticity (El-Husseini and Bredt 2002; Fukata and Fukata 2010; Korycka et al. 2012; Ohno et al. 2006).

The PAT ZDHHC7 targets various synaptic proteins such as neural cell adhesion molecules (Ponimaskin et al. 2008) or gamma-aminobutyric acid (GABA) receptors subtype A ($GABA_A$) (Naumenko and Ponimaskin 2018). On the other hand, $GABA_A$ receptor γ2 subunits are palmitoylated by the paralog ZDHHC3 but not by ZDHHC7; this is demonstrated in ZDHHC3 (GODZ) and ZDHHC7 (SERZ-β) mouse models (Kilpatrick et al. 2016). Via knockdown studies in cancer cells, ZDHHC7 and another paralog, ZDHHC21, were identified to palmitoylate the estrogen ERα, ERβ, progesterone (PR), and androgen (AR) sex steroid receptors (Pedram et al. 2012). The authors further revealed that ER-, PR-, and AR palmitoylation by both PATs (ZDHHC7 and ZDHHC21) are crucial for membrane trafficking and non-genomic/non-classical rapid responses to steroid hormones (Pedram et al. 2012). Such rapid signal transduction impacts neuroanatomical structures, synaptic transmission and plasticity, intracellular signaling cascades, and downstream gene expression (Balthazart and Ball 2006; Baudry et al. 2013; Ooishi et al. 2012). For instance, rapid ER-mediated signaling is involved in early hippocampal organization in a sex-specific manner. It requires rapid estradiol effects via ERα, which interacts with metabotropic glutamate receptors (mGluR) within caveolin 1 (CAV1)-generated microdomains (e.g., Boulware et al. 2005; Meitzen et al. 2012). Rapid ER signaling depends on the expression of both ZDHHC7 and ZDHHC21 (Meitzen et al. 2013; Tonn Eisinger et al. 2018). However, only ZDHHC7 increases also CAV1-palmitoylation and has widespread expression in cellular compartments, while ZDHHC21 appears to be not required for CAV1-palmitoylation and to be restricted to the Golgi apparatus (Tonn Eisinger et al. 2018). Moreover, only ZDHHC7 and CAV1 mRNAs, but not ZDHHC21 mRNA, differ sex-specifically at distinct developmental stages (Meitzen et al. 2017). This indicates a possible significance of ZDHHC7 with regard to sex differences in the brain.

Coupling of ERs to CAV-microdomains is found across the nervous system, among others in hippocampus and cortex (Meitzen et al. 2012; Spampinato et al. 2012). Particularly the medial prefrontal cortex (mPFC) is involved in the regulation of cognition, emotion, socio-affective, and visceromotor behaviors (Bandler et al. 2000; Damasio et al. 2000; Franklin and Chudasama 2012; Uylings et al. 2003) and is affirmed in its intrinsic sex-specificity. For example, GABAergic or estradiol-dependent glutamatergic transmission and synaptic plasticity are sex-specifically regulated in the mPFC (Galvin and Ninan 2014; Fernandez et al. 2015). In addition, mPFC has extensive connections with cortical and subcortical limbic areas including the hippocampus (Franklin and Chudasama 2012), forming a network that is highly sensitive to sex differences (Seney and Sibille 2014). Together, cortico-limbic sex-specificity affects neuroanatomy, microstructure, structural connectivity, and transmission between brain regions (Palanza and Parmigiani 2017; Zagni et al. 2016) as well as emotional/behavioral outcomes such as fear, anxiety, and mood (Brinton et al. 2008; Suzuki et al. 2013). However, the direct role of ZDHHC7 in brain (micro)structure, GABAergic/glutamatergic transmission, and behavior has, thus far, not been investigated.

In the current study, we hypothesized that ZDHHC7 deficiency could sex-specifically alter brain microstructure/connectivity, synaptic transmission and related proteins such as mGluR, synaptic plasticity, and the behavioral outcome. We, therefore, generated a mouse model with constitutive inactivation of the *Zdhhc7* gene and directly analyzed both male and female *Zdhhc7*$^{-/-}$ vs. wild-type mice using a set of

various methods such as behavioral characterization, electrophysiology, and neuroimaging.

Materials and methods

Generation of *Zdhhc7*-deficient mice

A detailed description of targeting construct design, various molecular biology methods, blastocyst injection, and CRE-mediated deletion of *Zdhhc7* exon 4 (essential for PAT activity),is given in the Online Resource. Briefly, based on the *Zdhhc7* wild-type locus (Fig. 1a), the *Zdhhc7* targeting construct contained a FRT-flanked neomycin-resistance cassette (NeoR) harboring one *lox*P site immediately 5′ to the proximal FRT site. This cassette replaced an 855 bp DNA fragment of the third intron (Fig. 1b). Between NeoR and the 5′ end of exon 4, 51 bp of intron 3 sequence remained. An additional *lox*P site was placed 59 bp downstream from exon 4 (in intron 4). The final targeting construct comprised a 2.2 kb upstream flanking region, the *lox*P site, the Frt-NeoR-PGK-Frt cassette, the 0.3 kb target region around exon 4, the second *lox*P site, and a 5.8 kb downstream flanking region, as depicted in Fig. 1b. Positively targeted CV19 ES cells (129 Sv x C57BL/6 J) were identified by Southern blot analysis using a 1.3 kb external probe (HR1; see Fig. 1c–f, Online Resource Suppl. Fig. 1), and verified using the 1.2 kb internal probe (SI; Fig. 1c). Subsequent injection of positively targeted ES cells into B6D2F1 blastocysts resulted in several high percentage male chimaeras, which were crossed to C57BL/6 J females for germ-line transmission of targeted exon 4 and verified by Southern blot analysis. Finally, successful inactivation of the *Zdhhc7* gene was achieved via excision of the Frt-NeoR-PGK-Frt cassette-exon 4 region flanked by *lox*P sites by crossing mice with total CRE-deleter transgenic mice, verified by Southern blot analysis (Fig. 1d, g, Online Resource Suppl. Fig. 2). Even if not (completely) degraded by nonsense-mediated decay (cf. Baker and Parker 2004), the predicted mRNA would encode a protein product that would be out of frame after 106 amino acids out of a total of 308 amino acids.

For qPCR-based validation of targeted exon 4 deletion, 14 mice (*Zdhhc7*$^{-/-}$ (KO) female: $n = 4$; wild-type (WT) female: $n = 4$; KO male: $n = 3$; WT male: $n = 3$) were decapitated under isoflurane anesthesia (CP Pharma, Burgdorf, Germany). Brains were immediately dissected and stored at – 20 °C in RNAlater (Life Technologies, Darmstadt, Germany). Total RNAs were extracted from left hemisphere mPFCs (representing the cortico-limbic network) following customized Trizol-based procedure (Direct-zol RNA MiniPrep Kit with ZR BashingBead Lysis Tubes (mixed) and DNase-I treatment; Zymo Research, Freiburg, Germany). After photometric assessment of total RNA (A260/A280 ratios), cDNAs were synthesized from 266 ng RNA per mouse using the High Capacity cDNA RT Kit (Life Technologies) as recommended. TaqMan Gene Expression Assays (*Zdhhc7*: Mm00505997_m1, spanning exons 4–5; endogenous control *Gapdh*: Mm99999915_g1; Life Technologies) and TaqMan Gene Expression Master Mix (Life Technologies) were used for qPCR in triplicate following the manufacturer's instructions (setup: Freedom EVO 150 system, Tecan, Crailsheim, Germany; qPCR instrument: Applied Biosystems 7900HT Real-Time PCR System, Life Technologies). Expression of the endogenous control was determined for calculation of ΔCt to reveal relative *Zdhhc7*-expression for WT vs. KO mice. In contrast to relative *Zdhhc7*-expression values within the expected range in WTs, these were completely absent in KO mice (Fig. 1h). This loss of amplification products that spanned exons 4–5 further confirmed the knockout of *Zdhhc7* exon 4.

Experimental animals

After establishing the *Zdhhc7* mouse line (more details in Online Resource), mice (available upon request) were examined with respect to their general health condition, reproduction, and potential signs of knockout induced burden or stress (severity assessment following german BfR guidelines). Comparison of *Zdhhc7* KO and heterozygous mice with WT conspecifics revealed normal range (WT-like) motor and sensory activity, reflexes, health, and reproduction. No signs of any burden or stress were observed under standard housing conditions in the central animal facility (ZTE) of the University of Münster. Heterozygous crosses were then utilized to produce KO and WT offspring for subsequent experiments. Initially, sets of mice underwent behavioral and electrophysiological phenotyping and additional sets were used for protein analyses and neuroimaging (described below). Experimental mice were weaned between postnatal weeks 3–4 and same sex littermates (KO and WT mice from the above-mentioned heterozygous crosses) were housed together in Makrolon Type II L cages ($37 \times 21 \times 14$ cm^3) with sawdust as bedding material and access to food and water ad libitum.

The presented work was in accordance with all current regulations covering animal experimentation in Germany and the EU (European Communities Council Directive 2010/63/EU). All experiments were approved by the local authority and the "Animal Welfare Officer" of the University of Münster. All efforts were made to minimize animal suffering as well as to reduce the number of animals used

in this study to a minimum necessary for reliable statistical analyses.

Behavioral testing

A total of 40 mice (WT female: $n=8$; KO female: $n=11$; WT male: $n=10$; KO male: $n=11$) were transferred to the experimental housing room at 9 weeks of age. Housing included controlled standard conditions with temperature at 21 °C (± 1 °C), humidity of 50% (± 10%), and a 12:12 h light–dark cycle (lights on at 6 am). After 1 week of acclimatization, behavioral testing started with a total of six different tests. Tests were performed in the following order (from least to most stressful): open-field test (OFT) at postnatal day (P) 70 to assess locomotor and anxiety-related behaviors, elevated plus-maze test (EPM) at P72 to again assess anxiety-related behavior, spontaneous alternation test (SAT) at P74 to assess spatial working memory, sociability test (SoT) at P76 to assess social exploration, object relocation and recognition test (ORR) at P78 to assess cognitive function, and forced swim test (FST) at P82 to assess behavioral despair as measure of depression-like behavior.

The OFT was conducted for 10 min in an 80 × 80 cm box which was illuminated with 190 lx in the center zone as described before (Ambrée et al. 2016).

The EPM was performed as described before (Ambrée et al. 2016). At the beginning of each test, the animal was placed in the center zone (brightly illuminated with 190 lx) with the head directed towards a closed arm. It could freely explore the maze for 5 min.

The SAT was performed as described before (Sakalem et al. 2017). The animals were placed into one arm and could freely move in the apparatus for 6 min. The sequence of entries was recorded by a trained observer blind to the genotype with an entry defined as all four limbs entering an arm.

The SoT was used to assess the exploration of an unfamiliar conspecific. It was conducted in a three-chambered apparatus as described before (Sakalem et al. 2017). It comprised two trials of 5 min each, one for habituation with empty wire cages, the other with an unfamiliar mouse and a ball as object control in the wire cages on opposite sides of the apparatus. Frequencies and time of exploration were recorded by a trained observer blind to the genotype using the ANY-maze software (Stoelting, Wood Dale, IL, USA). The percentage of social exploration was calculated as the exploration time of the conspecific in relation to the total exploration time of conspecific and object.

The ORR was performed in an open-field apparatus (40 × 40 × 40 cm) and consisted of six trials in total, three on each of two consecutive days. Each trial lasted 5 min. Initially, the mouse was placed in the front left corner, where it could freely explore the empty apparatus (habituation trial). After this, the mouse was returned to its home cage for 5 min. In the second trial, the object exploration trial, the mouse could explore two different inanimate novel objects (A + B) placed in the rear left and right corners 6 cm from the walls for 5 min. In the third trial, immediately following the second, object B was relocated from the rear to the front right corner (object relocation trial). The next day, the first two trials were completely identical as 24 h before (habituation and object exploration). In the last part, the object replacement trial, object B was replaced by a novel, unfamiliar object C, located at the exact same position as object B before. Throughout the experiments, the frequency and time each mouse spent exploring each object was manually recorded using ANY-maze by a trained observer blind to the genotype. Mice were considered to explore when their head faced towards and touched or sniffed the respective object. The number and time of object exploration were recorded. Percentage of recognition was calculated as the ratio of the amount of time spent exploring the relocated or the novel object in relation to the total time spent exploring both objects in the respective trial.

The FST to measure depressive-like behavior was performed in a glass cylinder (height: 28 cm, diameter: 13.5 cm; Roth) filled 15 cm high with tap water (21 ± 1 °C). Each mouse was placed in the water and the behavior was manually recorded for 6 min using ANY-maze to score immobility (floating: only small movement necessary to keep the head above water such as tail or single limb movement) and active time (swimming and struggling: climbing or jumping at walls) by an observer blind to the genotype of the animals. After the test, the mouse was briefly toweled and was put into a cage with half of the area under a heating lamp for 5 min before it returned to its home cage.

All tests were performed by the same experimenter. If not mentioned otherwise, all tests were automatically recorded using the tracking software (ANY-maze).

Electrophysiological recordings

After the behavioral tests at 12 weeks of age, a subset of 34 mice (WT female: $n=8$; KO female: $n=9$; WT male: $n=6$; KO male: $n=11$) was used for whole-cell patch recordings in mPFC slices. An additional 22 mice (WT female: $n=5$; KO female: $n=7$; WT male: $n=5$; KO male: $n=5$) were used at 11 weeks of age for extracellular recordings in hippocampal slices. All mice were decapitated under isoflurane anesthesia to immediately dissect their brains blinded to sex and genotype. Hippocampal and mPFC slice preparation and electrophysiological recordings were performed as described previously (Agarwal et al. 2014; Saffari et al. 2016; Wehr et al. 2017). Briefly, after transfer of brains into ice-cold oxygenated preparation solution, acute transverse mPFC slices (300 µm) or coronal hippocampal slices (300 µm) were cut and transferred into incubation chambers with warm

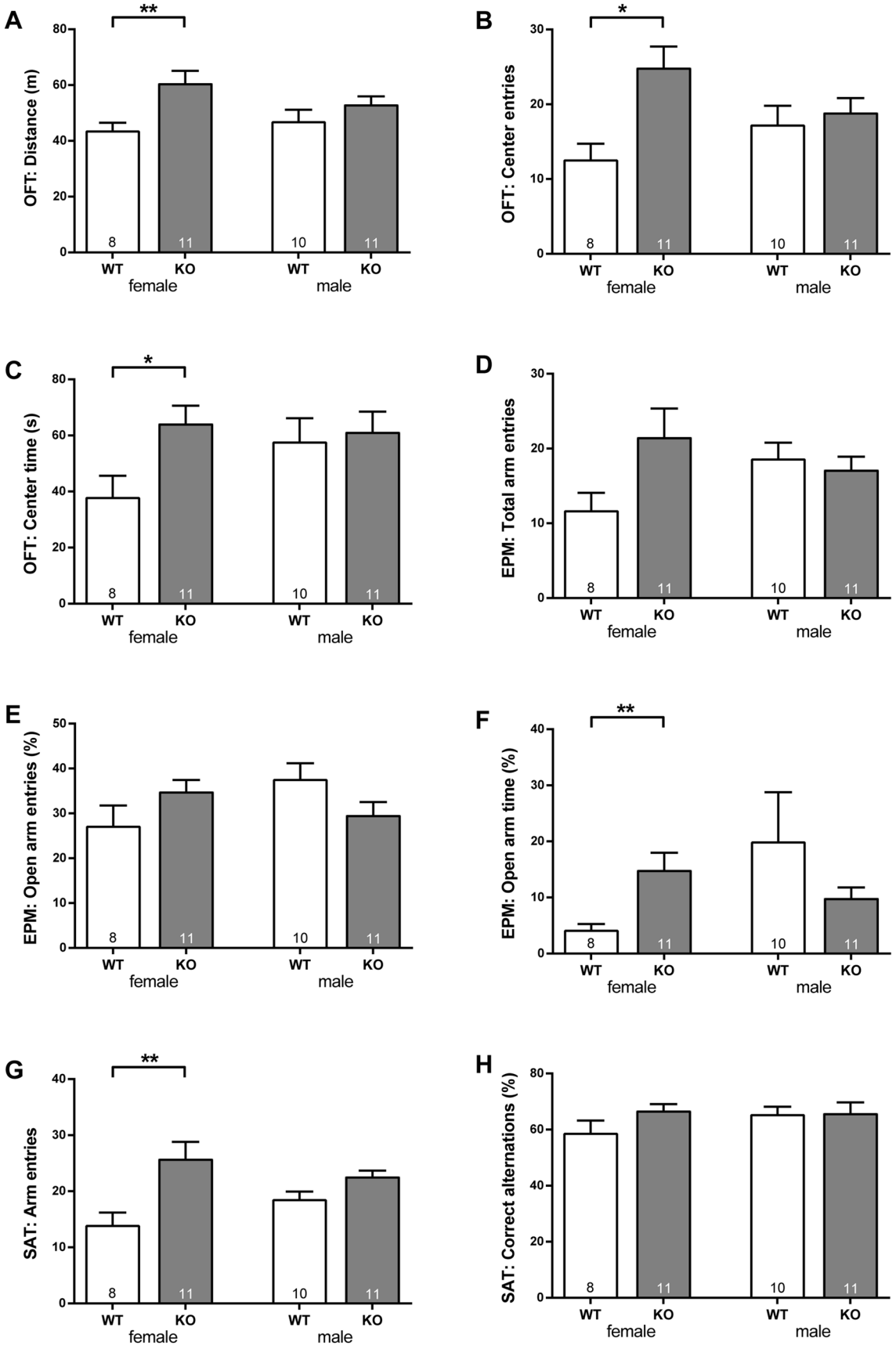
A
OFT: Distance (m)
**
B
OFT: Center entries
*
C
OFT: Center time (s)
*
D
EPM: Total arm entries
E
EPM: Open arm entries (%)
F
EPM: Open arm time (%)
**
G
SAT: Arm entries
**
H
SAT: Correct alternations (%)
8
11
10
11
WT
KO
female
male

◂**Fig. 2** Differential effects of *Zdhhc7*-deficiency on locomotor, anxiety-related, and cognitive behavior. Male and female *Zdhhc7* KO and WT mice were analyzed in the open-field test (OFT) (**a–c**), the elevated plus-maze test (EPM) (**d–f**), and the spontaneous alternation test (SAT) (**g, h**). **a** *Zdhhc7* KO females showed increased locomotor activity as indicated by the total distance traveled in the OFT. **b** Female KO mice also presented increased entries into the center of the open field and **c** spent more time therein indicating a reduction in anxiety-related behavior. **d** Number of arm entries as a measure of locomotor activity did statistically not differ. **e** There was no difference in the percentage of open arm entries in the EPM. **f** Percentage of time spent on the open arms of the EPM was significantly increased in female KO mice, once more suggesting a reduction in anxiety. **g** Increased number of alternations in the SAT in female and male KO mice. **h** No differences in the percentages of correct alternations were detected in the SAT. Male mice did not differ with respect to their genotype. Bars present group means (±SEM) with bottom numbers indicating sample sizes per group, asterisks depict the level of significance (*$p < 0.05$; **$p < 0.01$)

oxygenated artificial cerebrospinal fluid for a 1 h recovery period.

Whole-cell patch recordings of excitatory glutamatergic or inhibitory GABAergic synaptic transmission were assessed by recordings of postsynaptic currents (PSCs) of pyramidal neurons in the prelimbic area of the mPFC. Spontaneous inhibitory PSCs (sIPSCs) and spontaneous excitatory PSCs (sEPSCs) were recorded at holding potentials of − 70 mV for 5 min in the presence of 6-cyano-7-nitroquinoxaline-2,3-dione (10 µM) and 2-amino-5-phosphonopentanoic acid (40 µM) for sIPSC, or strychnine and bicuculline (10 µM each) for sEPSC. Spontaneous PSC recordings were followed by recordings of miniature inhibitory PSCs (mIPSCs) and miniature excitatory PSCs (mEPSCs) for 5 min after adding tetrodotoxin (0.5 µM) to the bath solution. Signals with amplitudes of at least two times above the background noise were selected, while patches with serial resistance of > 20 MΩ, a membrane resistance < 0.8 GΩ, or leak currents of > 150 pA were excluded (data acquisition and analysis by pClamp 10.0 (Molecular Devices, Sunnyvale, CA), MiniAnalysis [SynaptoSoft, Decatur, GA) and Prism 6 (GraphPad, San Diego, CA)]. In addition, decay kinetics were analyzed as described previously (Medrihan et al. 2008) based on mIPSC and mEPSC recordings (Jonas et al. 1998; Nabekura et al. 2004). Extracellular recordings of hippocampal slices were performed as described by Agarwal et al. (2014) by stimulating Schaffer collaterals with the stimulation electrode placed in the stratum radiatum at the CA3/CA1 junction. To study short-term potentiation (STP) and long-term potentiation (LTP), extracellular stimulation induced responses were recorded then in the stratum radiatum in the CA1 region.

Protein analyses

A set of 16 mice (female KO–WT littermates: $n = 4$; male KO–WT littermates $n = 4$; at P89–120) was decapitated under isoflurane anesthesia to immediately remove brains, dissect mPFCs, and snap froze them in liquid nitrogen. Two exemplary candidate proteins related to GABAergic/glutamatergic synaptic transmission were selected for protein analyses. First, the GABA(B) receptor 1 ($GABA_BR1$), since $GABA_BRs$ have been shown to be enriched in the limbic system and to be involved in regulating anxiety-/depression-related behavior (Cryan and Kaupmann 2005), whereas $GABA_A$ receptor γ2 subunits are palmitoylated by ZDHHC3 but not by ZDHHC7 (Kilpatrick et al. 2016). Second, we selected mGluR2 (enriched in mPFC and hippocampus, strongly involved in regulating glutamatergic/GABAergic transmission; Mateo and Porter 2007; Pilc et al. 2008; Wright et al. 2013). Both proteins were investigated with respect to putatively ZDHHC7-related palmitoylation in the *Zdhhc7* KO and WT mice using the acyl-biotinyl exchange (ABE) methodology as described previously by Steinke et al. (2015). After ABE, protein samples were subjected to SDS-PAGE followed by western blot analysis using as primary antibodies rabbit polyclonal anti-GABA(B)R1 (cat. no. 3835, Cell Signaling Technology, Frankfurt a. M., Germany; dilution 1:1000) and rabbit polyclonal anti-mGluR2 (cat. no. AGC-011 Alomone Labs, Jerusalem, Israel; dilution 1:200). Target proteins were visualized by chemiluminescence using goat anti-rabbit IgG (H + L) secondary antibody, HRP conjugate (ThermoFisher Scientific). Images were taken with the Fusion SL Imager (Vilber Lourmat, Eberhardzell, Germany). For densitometry analyses, the signal intensity of each unsaturated band was assessed and the gel background removed individually with the ImageJ tool (version 1.51j8, Wayne Rasband, NIH USA; http://imagej.nih.gov/ij). The coefficient of palmitoylation variation was calculated as the ratio of ABE-band values to control values before normalizing to WT controls.

Neuroimaging (MR scanning and DTI fiber tractography)

A total of 14 mice (female KO–WT littermates: $n = 4$; male KO–WT littermates $n = 3$; at P121–127) were deeply anesthetized intraperitoneally (Xylazin 10 mg/kg and Ketamin 100 mg/kg body weight) and transcardially perfused with phosphate buffered saline (PBS, 0.1 M, pH 7.0) and afterwards with 4% paraformaldehyde (PFA). After immediate decapitation, brains were removed and kept in 4% PFA for 4 days at RT, followed by washing and incubation for additional 24 h in aqueous solution of contrast agent (2 mmol/L Magnevist, Bayer Pharma AG, Berlin, Germany). Brains were embedded into small plastic tubes (5 ml syringe) in

1% agar enriched with contrast agent (2 mmol/L Magnevist) and scanned on a 9.4 T small animal imaging system with a 0.7 T/m gradient system (Biospec 94/20, Bruker Biospin GmbH, Ettlingen, Germany) and a helium-cooled surface coil (CryoProbe, Bruker Biospin). Anatomical MR images were acquired with a T2 weighted 3D RARE protocol (TR/TE 2000/73 ms, two averages, 384 × 384 × 256 matrix, FOV 1.6 cm^3, 40 × 40 × 60 μm^3 voxel size; Fig. 5a1). Diffusion tensor data were acquired with an eight-segment EPI-DTI protocol (TR/TE 9000/34 ms) with 30 diffusion directions ($b = 1000$ s/mm^2, diffusion gradient duration = 4 ms, diffusion gradient separation = 10 ms, and eight experiments/direction) and five B0 images, FOV 1.6 × 1.4 cm^2, 160 × 140 matrix, in plane resolution 100 μm^2, slice thickness 200 µm (Fig. 5a2).

DTI fiber tractography was performed using the DTI&Fiber Tool (Kreher et al. 2006; https://www.uniklinik-freiburg.de/mr-en/research-groups/diffperf/fibertools.html). The mouse brain atlas (Paxinos and Franklin 2013) was used to define the left hippocampus as region of interest (ROI) for each mouse blind to sex and genotype. The ROI was set then as start mask to apply streamline DTI fiber tracking (implemented FACT algorithm according to Mori et al. 1999) with default parameters related to fractional anisotropy (FA) [start criterium: FA > 0.25, Tr(D) < 0.0016; stop criterium: FA > 0.15, Tr(D) < 0.002; max. angle = 53.1°; min. voxel = 5]. Hippocampal volumes, FA values within the ROIs, and fiber statistics were determined.

To further identify putatively connecting fibers from hippocampus to prelimbic (PL)/infralimbic (ILA) mPFC subareas, the Allen Mouse Brain Connectivity Atlas (2011) (Oh et al. 2014; http://connectivity.brain-map.org/) was used. This open database provides axonal projection data of all brain subregions based on individually injected tracer in different mouse strains. In wild-type C57BL/6 J mice, the database revealed axonal projections between hippocampus and PL/ILA. These turned out as prominent and converging axon bundle originating from a medioventral CA subregion in the hippocampus (Online Resource Suppl. Fig. 3a–e). The spatial position of this region was chosen to define an analog second ROI in four consecutive coronal DTI slices in *Zdhhc7* KO and WT mouse brains (Online Resource Suppl. Fig. 3f–k). ROI-based Mori fiber tracking (Online Resource Suppl. Figs. 3 l–n, 4, and 5) was then used as aforementioned to determine fiber statistics for the medioventral hippocampal CA region in male and female *Zdhhc7* KO vs. WT mice.

Statistical analyses

All statistical tests were computed using SPSS (version 25, IBM Corp., Ehningen, Germany) or Prism (version 5.0, GraphPad Software, San Diego, CA, USA). Data sets were checked for normal distribution by one-sample Kolmogorov–Smirnov and Shapiro–Wilk tests. When not or partly not normally distributed, the impact of *Zdhhc7*-deficiency, that is KO vs. WT, was analyzed using the Mann–Whitney *U* test for non-parametric testing separately in males and females, respectively. Otherwise, if normally distributed, the Student's *t* test was applied analogously. The level of statistical significance was set to $\alpha = 0.05$, but adjusted individually following Bonferroni correction for multiple testing in case of hippocampal fiber statistics: testing FA data sets three times (minimal, maximal, and mean FA) resulted in adjusted $\alpha = 0.017$; testing hippocampus or medioventral hippocampal CA region data sets two times each (maximal and mean fiber length) resulted in adjusted $\alpha = 0.025$, respectively. All data were presented as group means (± SEM).

Results

Zdhhc7 KO increases locomotion but reduces anxiety-related behavior only in female mice

To investigate the effect of *Zdhhc7*-deficiency on locomotor, anxiety-related, social, and despair behaviors, as well as learning and memory, we analyzed KO and WT mice of both sexes in a series of behavioral tests. In the OFT, female KOs traveled a significantly longer distance than WTs (Fig. 2a, $t = -3.05$, $df = 17$, $p = 0.007$), while males did not differ between the genotypes ($p > 0.05$). Regarding anxiety-related behavior, female KOs displayed significantly more entries into the center (Fig. 2b, $t = -3.24$, $df = 17$, $p = 0.005$) and also spent more time therein (Fig. 2c, $t = -2.66$, $df = 17$, $p = 0.017$). While the first measure could be a result of increased locomotor activity, the latter indicates reduced anxiety-related behavior in female KOs. Male mutants, in contrast, showed comparable levels of anxiety-related behavior compared to the WT controls (Fig. 2b, c, all $p > 0.05$).

In the EPM, alternation between the arms as indicator of locomotion did not differ statistically between mutants and WTs of both sexes (Fig. 2d, all $p > 0.05$). Regarding anxiety-related behavior, female KOs also did not differ from WT mice in relative open arm entries (Fig. 2e, $p > 0.05$), while they spent significantly more time in the open arms than WTs (Fig. 2f, $t = -3.29$, $df = 12.153$, $p = 0.006$); this supports the findings from the OFT that female KOs showed reduced anxiety-related behavior. In males, relative open arm entries and relative time in open arms did not differ statistically between KOs and WTs (Fig. 2e, f, all $p > 0.05$), suggesting that *Zdhhc7* is more relevant for anxiety-related behavior in female mice.

To assess spontaneous alternations as a measure of spatial working memory (Hughes 2004), we applied the SAT. Female and male KO mice showed significantly more

alternations than WTs (Fig. 2g, female: $t=-2.95$, $df=17$, $p=0.009$; male: $t=-2.39$, $df=19$, $p=0.027$). With regard to the percentage of correct alternations, there were no differences between KO and WT in either sex (Fig. 2h, all $p>0.05$). In addition, no differences were observed with respect to sociability, behavioral despair, and object relocation and recognition (Online Resource Suppl. Fig. 6). Thus, in the above-mentioned behavioral domains, *Zdhhc7*-deficiency affects locomotion in both females and males, yet anxiety-related behaviors are affected exclusively in female mice.

Zdhhc7 KO differentially alters the excitatory and inhibitory synaptic transmissions in mPFC of male and female mice

Subsequently, we tested excitatory glutamatergic synaptic transmissions in prelimbic mPFC of female and male *Zdhhc7* KO and WT mice (Fig. 3). In female mutants, the frequency of mEPSC, but not sEPSC was significantly depressed (mEPSC $U=471.0$, $z=2.12$, $p=0.033$; Fig. 3b, d). In male mutants, the frequencies of both sEPSC and mEPSC were similarly depressed compared to frequencies in the respective WT controls (sEPSC $t=2.31$, $df=29$, $p=0.028$, mEPSC $U=320.0$, $z=2.25$, $p=0.024$; Fig. 3b, d), whereas the amplitudes did not differ statistically in KOs vs. WTs in both sexes (all $p>0.05$; Fig. 3a, c). In addition, the mEPSC decay time of male KOs was prolonged compared to the decay time in WTs ($U=13.0$, $z=-2.16$, $p=0.030$; Fig. 3e). In contrast, there was no alteration of decay time in female mice between genotypes (18.3 ± 3.5 ms in WT vs. 18.2 ± 3.1 ms in KOs; $p>0.05$; Fig. 3e). In sum, the impact of *Zdhhc7*-deficiency on excitatory synaptic transmission is more pronounced in male than in female mice.

Analysis of inhibitory GABAergic synaptic transmission of *Zdhhc7* mice revealed distinct sex-specific differences (Fig. 4). It is worth mentioning that the average amplitude of sIPSC were observed to be lower in female WT as compared to amplitudes in male WT animals (Fig. 4a). Strikingly, both sIPSC and mIPSC amplitudes were significantly upregulated in female KOs compared to the amplitudes in female WTs (sIPSCs $U=163.5$, $z=-2.36$, $p=0.017$, Fig. 4a; mIPSCs $t=3.07$, $df=57$, $p=0.003$, Fig. 4c). The average amplitudes of sIPSCs reached comparable values in male and female *Zdhhc7* mutant mice. On the other hand, the frequencies of both sIPSCs ($t=2.81$, $df=42$, $p=0.008$; Fig. 4b) and mIPSCs ($t=2.43$, $df=46$, $p=0.019$; Fig. 4d) were downregulated in male KOs compared to the frequencies in male WTs. Moreover, current decay of mIPSCs in female mutants was significantly slower compared to the same parameter in WTs (15.6 ± 0.6 ms in WTs vs. 19.8 ± 2.2 ms in KOs, $U=113.0$, $z=-2.15$, $p=0.032$; Fig. 3f), while there was no significant difference between genotypes in male mice (18.6 ± 2.1 ms in WT vs. 18.14 ± 2.4 ms in KOs; $p>0.05$; Fig. 3f). Subsequently, we also explored palmitoylation of $GABA_BR1$ and mGluR2 utilizing the ABE method. No altered palmitoylation was statistically apparent in the *Zdhhc7*-deficiency mice vs. WT mice in both sexes and for both proteins (Online Resource Suppl. Fig. 7; both $p>0.05$). Hence, while *Zdhhc7*-deficiency impaired excitatory synaptic transmission in both sexes but stronger in male mutants, it affected inhibitory transmission in both sexes inversely in a distinctly sex-specific manner.

Synaptic plasticity is significantly impaired at Schaffer collateral CA1 synapses of both female and male *Zdhhc7* mutants

We then tested the hippocampal LTP induced at Schaffer collateral CA1 synapses. In female KOs vs. WTs, both the input–output curves as well as the paired-pulse facilitation were unaltered, suggesting that there were no genotype-specific changes in basal excitability (Online Resource Suppl. Fig. 8). However, after high-frequency stimulation (HFS), STP, determined as the average of responses in the first 5 min after HFS, was significantly decreased in female mutants ($U=25.0$, $z=2.50$, $p=0.012$; Fig. 4e, f). Similarly, the magnitude of LTP, determined as the average of responses between 50 and 60 min, was also significantly decreased in female mutants ($U=100.0$, $z=3.74$, $p\leq0.001$; Fig. 4g). Similar to the results obtained in females, both the input–output curves and paired-pulse facilitation were unaltered in male KOs vs. WTs (Online Resource Suppl. Fig. 8). In addition, the magnitudes of both STP and LTP were significantly decreased in male mutants vs. WTs ($U=25.0$, $z=2.50$, $p=0.007$, $t=13.95$, $df=18$, $p\leq0.001$; Fig. 4h–j). Collectively, these data show that deficiency of *Zdhhc7* similarly impaired LTP in the hippocampus of both female and male animals.

Zdhhc7-deficiency alters the hippocampal fiber structures in male and female mice

Finally, we measured effects of *Zdhhc7*-deficiency on hippocampus using MRI and DTI fiber tractography. While hippocampal volumes, average fiber numbers, as well as mean and maximum FA values were similar between genotypes of both sexes (all $p>0.05$; Online Resource Suppl. Fig. 9), the minimal FA values appeared notably low in female WTs (Fig. 5b). *Zdhhc7*-deficiency altered this finding, namely female KOs revealed significantly higher minimal FA values ($t=$-3.69, $df=6$, nominal $p=0.010$, Bonferroni corrected $p=0.031$; Fig. 5b), resulting in values equaling those of male mice. In contrast, *Zdhhc7*-deficiency did not statistically affect minimal FA in male KOs vs. WTs (Fig. 5b; $p>0.05$). With respect to hippocampal fiber statistics, only

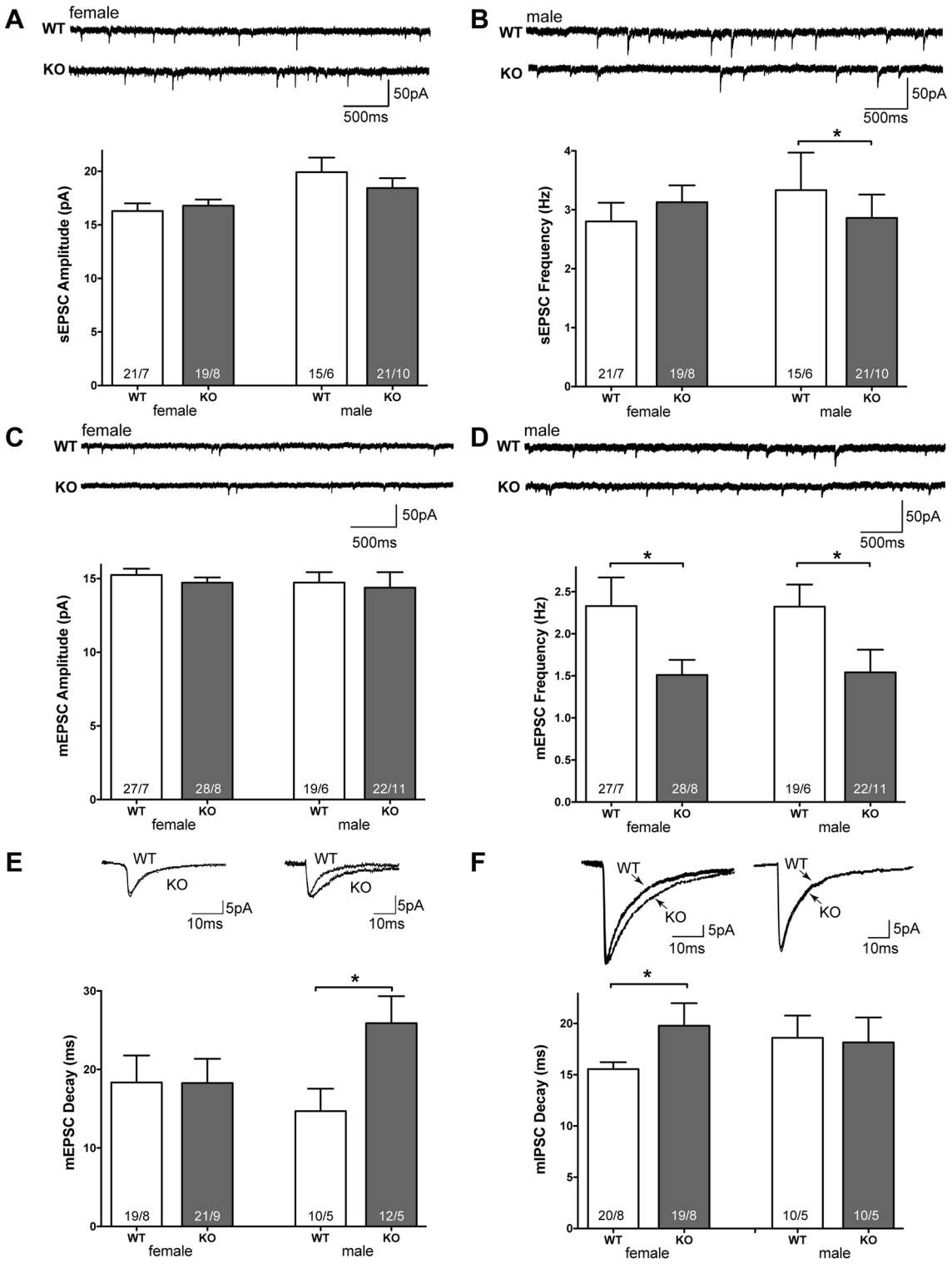

trend effects of sex-specificity were detectable. Mean fiber length was, by trend, shorter in female KOs than in female WTs ($t = 2.79$, $df = 6$, nominal $p = 0.031$, Bonferroni corrected $p = 0.063$; Fig. 5c), but not statistically different in males ($p > 0.05$). Maximal fiber length was. by trend, shorter in male KO mice vs. WT mice ($U = 0.0$, $z = -1.96$, nominal $p = 0.050$, Bonferroni corrected $p = 0.100$; Fig. 5d) but not in females ($p > 0.05$). In summary, hippocampal microstructure was affected by *Zdhhc7*-deficiency in a moderately sex-specific manner.

In contrast, subregional analyses of the hippocampal medioventral CA revealed strong effects of

◂**Fig. 3** Differential effects of *Zdhhc7*-deficiency on excitatory synaptic transmission and decay times in mPFC. **a** Upper part: sample traces of spontaneous excitatory postsynaptic currents (sEPSCs) in mPFC of female WT and KO mice; lower part: averaged amplitudes of sEPSCs in layer II pyramidal neurons of prelimbic mPFC of female (left) and male (right) WT and KO mice. **b** Upper: sample traces of sEPSCs in mPFC of male WT and KO mice; lower: averaged frequency of sEPSCs of female (left) and male (right) WT and KO mice. **c** Upper: sample traces of miniature excitatory postsynaptic currents (mEPSCs) in PFC of female WT and KO mice; lower: averaged amplitudes of mEPSCs of female (left) and male (right) WT and KO mice. **d** Upper: sample traces of mEPSCs in PFC of male WT and KO mice; lower: averaged frequency of mEPSCs of female (left) and male (right) WT and KO mice. **e** Upper part: comparison of the shape of mEPSCs of female (left) and male (right) WT and KO mice; lower: averaged decay time of mEPSCs of female (left) and male (right) WT and KO mice. **f** Upper: comparison of the shape of miniature inhibitory postsynaptic currents (mIPSCs) of female (left) and male (right) WT and KO mice; lower: averaged decay time of mIPSCs of female (left) and male (right) WT and KO mice. Bars represent group means (± SEM) with bottom numbers indicating sample sizes per group (*n*/*N*: recordings/total number of animals), asterisks depict the level of significance (*$p < 0.05$)

Zdhhc7-deficiency, yet similar in both sexes. In WT mice, fibers were longer and projected roughly towards mPFC (Fig. 5e), while in KOs, fibers were shorter and remained predominantly within the hippocampal medioventral area (Fig. 5f). This finding was consistent for all KO and WT mice of both sexes (Online Resource Suppl. Figs. 4, 5). Statistically, KOs of both sexes had significantly shorter mean fiber length (females: $t = 6.25$, $df = 6$, nominal $p = 0.001$, Bonferroni corrected $p = 0.002$; males: $t = 7.16$, $df = 4$, nominal $p = 0.002$, Bonferroni corrected $p = 0.004$; Fig. 5g) and shorter maximal fiber length (females: $t = 4.25$, $df = 6$, nominal $p = 0.005$, Bonferroni corrected $p = 0.011$; males: $t = 9.67$, $df = 4$, nominal $p = 0.001$, Bonferroni corrected $p = 0.001$; Fig. 5h). However, fiber numbers did not differ statistically between genotypes of both sexes (Online Resource Suppl. Fig. 9; both $p > 0.05$). Compared to the mild but sex-specific effects on whole hippocampus, deficiency of *Zdhhc7* impaired subregional hippocampal medioventral CA strongly but similarly in both female and male animals.

Discussion

Our data demonstrated for the first time that *Zdhhc7*-deficiency caused alterations of brain structure and function on a system level. Mutant mice of both sexes displayed impairments that included structural connectivity from hippocampus to mPFC (Fig. 5e–h), LTP-based synaptic plasticity in hippocampus (Fig. 4e–j), and miniature excitatory transmission in mPFC (Fig. 3d). Interestingly, all three findings appeared to be directly linked. Indeed, hippocampus and mPFC are structurally connected in mice (Franklin and Chudasama 2012; Allen Mouse Brain Connectivity Atlas: Online Resource Suppl. Fig. 3), which was substantiated by MRI–DTI data obtained from our *Zdhhc7* WT mice (Fig. 5e–h; Online Resource Suppl. Figs. 4, 5). Moreover, early experiments in rats characterized an anatomical hippocampus–mPFC pathway to be an excitatory glutamatergic connection, which also expresses LTP (Doyère et al. 1993; Jay et al. 1996). More recent experiments in mice also identified a monosynaptic hippocampus–mPFC pathway to likely be a glutamatergic connection (Tripathi et al. 2016). Finally, excitatory glutamatergic function could be shown to be directly related to LTP as reviewed by Lynch (2004). Such a hippocampus–mPFC pathway might be structurally altered in *Zdhhc7* inactivated mice; this is hinted at by our neuroimaging results. As a consequence, this might have led to the impaired excitatory glutamatergic function and the subsequent decreased LTP that our results revealed.

However, all other *Zdhhc7*-deficiency underlying alterations in brain structure, function, and behavior appeared in a distinct sex-specific manner. Male *Zdhhc7* mutants displayed additional impaired excitatory function (sEPSC frequency), slower excitatory decay times, reduced inhibitory transmission, and only slightly increased locomotion. In contrast, female *Zdhhc7* mutants revealed reduced anxiety combined with distinctly increased locomotion as well as increased inhibitory transmission, inhibitory decay time, and minimal hippocampal FA values. Thus, sex-specific differences due to *Zdhhc7*-deficiency were pronounced as hypothesized and discussed below.

The impact of *Zdhhc7* deficiency on male mice

Meitzen et al. (2017) demonstrated that ZDHHC7 is concordantly regulated with CAV1 with respect to development and sex-specificity of the brain. They assumed that normal excitatory glutamatergic transmission in adult male brains might depend on a functional ZDHHC7/CAV1-ERα pathway. Decreased CAV1 might then lead to diminished transmission (Meitzen et al. 2017). If this assumption holds true also for decreased ZDHHC7, *Zdhhc7*-deficiency might lead to diminished transmission as well. It might be even more likely, since ZDHHC7 is involved in the regulation of CAV1 function via increasing its palmitoylation (Tonn Eisinger et al. 2018). Indeed, in the present study, the frequencies of sEPSC and mEPSC were reduced and decay times prolonged in male mutants vs. WTs (Fig. 3b, d, e), indicating changes in the subunit composition of different glutamatergic postsynaptic receptors. On the other hand, structural alteration of the hippocampus–mPFC pathway might have led to the diminished transmission as discussed above (Doyère et al. 1993; Jay et al. 1996; Lynch 2004; Tripathi et al. 2016). However, the observation of stronger impairments in male *Zdhhc7*-deficient mice (in contrast to female mutants) suggests rather a combination of both structural and functional

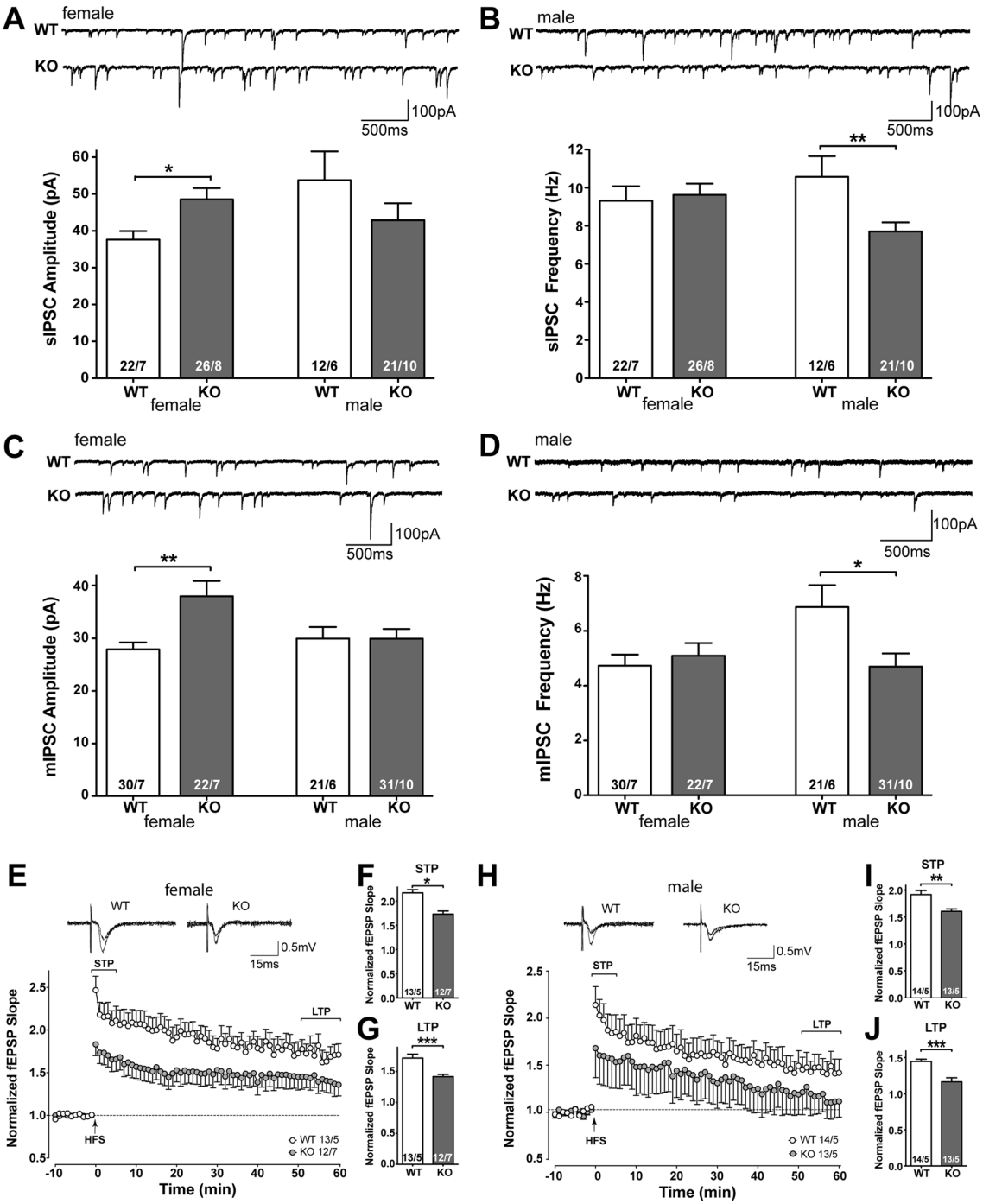

ZDHHC7/CAV1–ERα pathway effects to diminish glutamatergic transmission.

Interestingly, the aforementioned relation between excitatory glutamatergic function and LTP is mainly based on mGluRs (Lynch 2004). MGluRs functionally interact with ERs through pairing with different CAVs (e.g., Boulware et al. 2005; Meitzen et al. 2012); this seems to be both CAV specific and tissue specific. For example, CAV1 couples mGluR1 with ERα in hippocampus, and mGluR5 with ERα in striatum. In contrast, CAV3 couples mGluR2 with ERα and ERβ in hippocampus, and mGluR3 with ERα and ERβ in striatum (Boulware and Mermelstein 2009; Meitzen and Mermelstein 2011). In all cases, ERs are palmitoylated; thus, the coupling we observed—particularly the first example of CAV1-mGluR1-ERα—strongly resembles the aforementioned ZDHHC7/CAV1–ERα pathway suggested by Meitzen et al. (2017). Therefore, it is plausible that *Zdhhc7*-deficiency impairs

◂**Fig. 4** Differential effects of *Zdhhc7*-deficiency on inhibitory synaptic transmission in mPFC and on synaptic plasticity in hippocampal areas. **a** Upper part: sample traces of spontaneous inhibitory postsynaptic currents (sIPSCs) in mPFC of female WT and KO mice; lower part: averaged amplitudes of sIPSCs in layer II pyramidal neurons of prelimbic mPFC of female (left) and male (right) WT and KO mice. **b** Upper: sample traces of sIPSCs in PFC of male WT and KO mice; lower: averaged frequency of sIPSCs of female (left) and male (right) WT and KO mice. **c** Upper: sample traces of miniature inhibitory postsynaptic currents (mIPSCs) in mPFC of female WT and KO mice; lower: averaged amplitudes of mIPSCs of female (left) and male (right) WT and KO mice. **d** Upper: sample traces of mIPSCs in PFC of male WT and KO mice; lower: averaged frequency of mIPSCs of female (left) and male (right) WT and KO mice. **e** Long-term potentiation (LTP) at the SC-CA1 synapse in female WT and KO mice. Insets show sample traces of responses before and after high-frequency stimulation (HFS). Slopes of fEPSP were normalized to baseline and plotted against time. Time point 0 represents HFS application (arrow). **f** Short-term potentiation (STP) magnitude was significantly impaired in KO mice when compared to WT mice. **g** LTP magnitude was significantly impaired in KO mice vs. WT mice. **h** LTP at the SC-CA1 synapse in male WT and KO mice. Insets show sample traces of responses before and after HFS. **i** STP magnitude was significantly impaired in KO mice when compared to WT mice. **j** LTP magnitude was significantly impaired in KO mice vs. WT mice. (*n*/*N*:*n* = recordings, *N* = total number of animals). Bars represent group means (± SEM) with bottom numbers indicating sample sizes per group (*n*/*N*: recordings/total number of animals), asterisks depict the level of significance (*$p < 0.05$; **$p < 0.01$; ***$p < 0.001$)

excitatory glutamatergic function via mGluR candidates as shown in the present study (Fig. 3). However, one promising candidate, the mGluR2 (Mateo and Porter 2007; Pilc et al. 2008; Wright et al. 2013), was not differentially palmitoylated in female or in male WT vs. KO in our study. This suggests that other candidates might be responsible and requires systematic testing in subsequent analyses.

The stronger impairments observed in male mutants might also be due to an involvement of both ERα and ERβ in the modulation of pre- and postsynaptic glutamatergic signaling as shown by Oberlander and Woolley (2016). In contrast, in female *Zdhhc7* mutants less impairment of glutamatergic function was observed, maybe due to the fact that no ERα-involvement was detected in pre- and postsynaptic glutamatergic signaling (Oberlander and Woolley 2016).

Palmitoylated ERs have also been shown to be associated with GABAergic neurons in hippocampus (e.g., Hart et al. 2007). In addition, estradiol affects the GABAergic synaptic transmission in the developing hippocampus (Wójtowicz et al. 2008). In adolescent male mice, GABAergic signaling has been shown to be prominent in the prelimbic mPFC (Fernandez et al. 2015). These data led to the discovery that ERα is required for the masculinization of GABAergic neurons (Wu and Tollkuhn 2017). In the current study, not only glutamatergic, but also GABAergic transmissions were compromised in male *Zdhhc7* mutants (Fig. 4b, d). As a result—although the palmitoylation of $GABA_BR1$ was unaltered (Online Resource Suppl. Fig. 9)—the loss of ZDHHC7-mediated palmitoylation of ER by embryonic *Zdhhc7* deficiency might be responsible for the observed decreased inhibitory GABAergic transmission of male mutants in the present study.

The impact of *Zdhhc7* deficiency on female mice

Meitzen et al. (2017) reported that ZDHHC7 and CAV1 are abundant in developing (neonatal) rat hippocampi, but are decreased in hippocampi of adult females. Consistent with this, Oberlander and Woolley (2016) identified ERβ and GPER1 to be important for pre- and postsynaptic glutamate signaling in young adult females. However, only ERβ depends on palmitoylation and thus on the presence of ZDHHC7 (Meitzen et al. 2013; Pedram et al. 2012). If these observations also apply to mice, then *Zdhhc7*-deficiency should mainly affect the early life stages of females. In contrast, in males *Zdhhc7*-deficiency should affect adults as well. Therefore, it is plausible to assume that the impact of *Zdhhc7*-deficiency on females should be less pronounced. Our findings regarding excitatory glutamatergic transmission supported this assumption; females were less impaired than males (see above). However, all other *Zdhhc7*-deficiency-induced phenotypes were more pronounced in female compared to male mutants (Figs. 2a–c, f, g; 3f; 4a, c, e–g; 5b, c), which initially seemed counterintuitive.

Boulware et al. (2005) identified rapid estradiol actions via membrane ER-mGluR coupling that regulate phosphorylation of cAMP response element-binding (CREB) protein only in neonatal hippocampi of female but not male animals. Moreover, appropriate regulation of CREB phosphorylation via ERα/ERβ coupling to mGluR in female hippocampal neurons was crucial for the development of a normal female-specific hippocampus organization (Boulware et al. 2005). This physiological regulation was eliminated when neonatal females were exposed to testosterone/estradiol that led to a masculinization of female brains (Meitzen et al. 2012). Since ZDHHC7 is necessary for ERα/ERβ palmitoylation, constitutive inactivation of *Zdhhc7* already affecting the embryonic stage as observed in the present study, might possibly impair this female-specific pathway of hippocampus organization. Instead, *Zdhhc7* deficiency might favor male-specific pathways and signaling, similar to neonatal exposure to testosterone/estradiol (Meitzen et al. 2012). Indeed, in the present study, female *Zdhhc7* mutants displayed altered behavior, inhibitory GABAergic transmission, and hippocampal minimal FA values that appeared in a more male-typical pattern (c.f. Figs. 2c, f, 4a, 5b). It was previously suggested that changes in FA values could be caused by alterations in brain structure and organization as a result of myelination, neurite alignment, or axonal density (Anacker

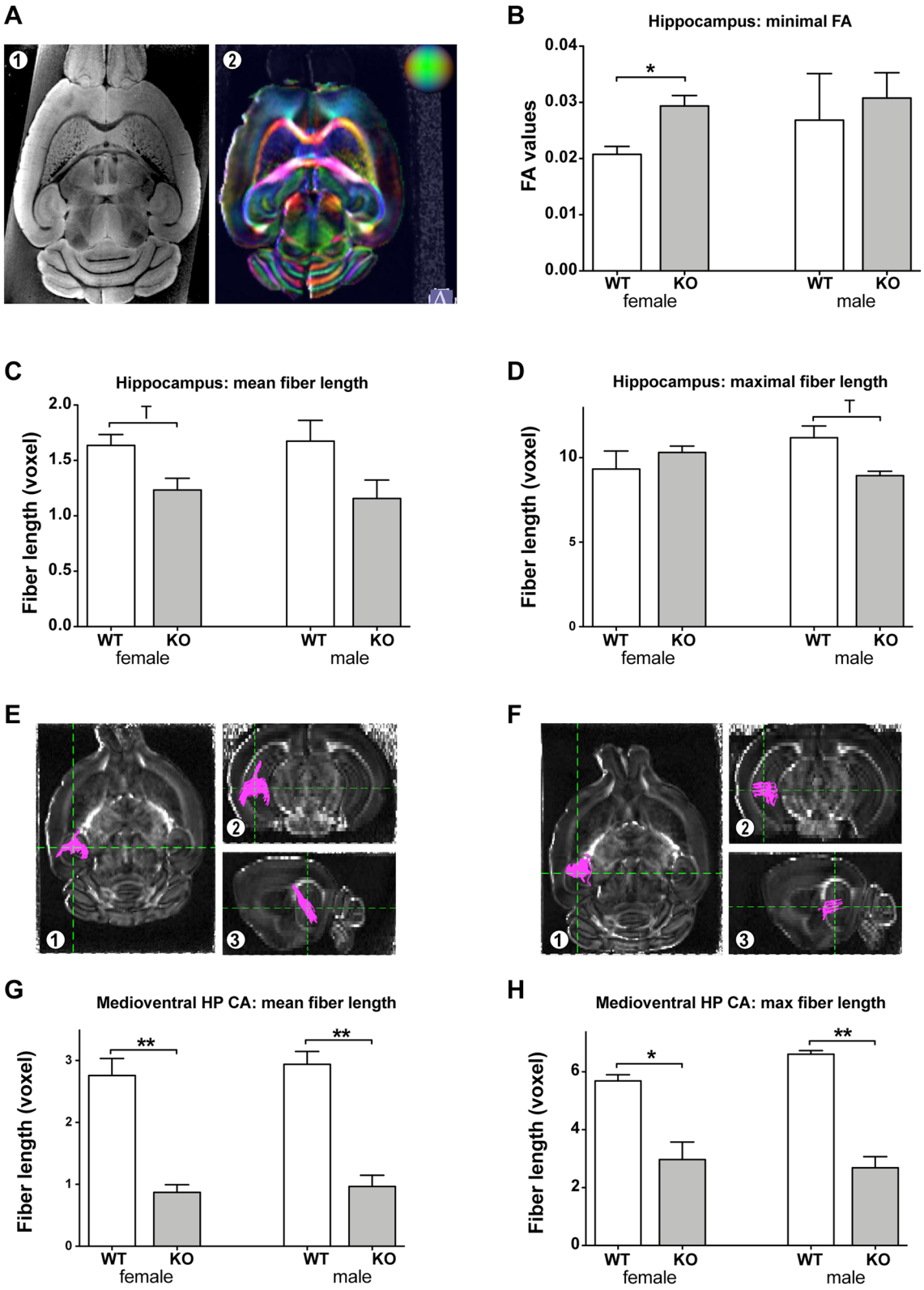

et al. 2016). Enhancement of such structures and organization initially increases FA (Anacker et al. 2016), whereas ongoing network formation in later life stages should slightly decrease FA in gray matter such as the hippocampus (Hammelrath et al. 2016). On the other hand, short-term motor-skill training already can increase hippocampal FA in mice

◂**Fig. 5** Differential effects of *Zdhhc7*-deficiency on hippocampal microstructure. **a** MRI- and DTI-based images of fixated mouse brains to obtain anatomical and fractional anisotropy (FA) data. (**1**) Illustrates a T2w 3D anatomical image in axial plane ($40\times40\times60$ µm^3 voxel size) and (**2**) a DTI-MRI colour-coded FA map in axial plane (30 diffusion directions, $100\times100\times200$ µm^3 voxel size). Major diffusion directions are indicated by red = left–right, green = anterior–posterior and blue = rostral–caudal. **b** Hippocampal FA analysis disclosed significantly higher minimum FA values in female KOs vs. WTs. **c** DTI fiber tracking revealed mean fiber length that was by trend (*T*; see statistics below) shorter in female KO vs. WT mice, whereas **d** maximal fiber length was by trend shorter in male KOs vs. WTs. **e, f** DTI&Fiber Tool-based images of fixated mouse brains to obtain Mori fiber tracking data used to analyze structural connectivity between medioventral hippocampal CA and mPFC. **e** Illustrates a *Zdhhc7* WT mouse compared to **f** a *Zdhhc7* mutant mouse, both in the different imaging planes axial (**1**), coronal (**2**), and sagittal (**3**). Corresponding fiber statistics of the medioventral hippocampal CA revealed significantly reduced mean (**g**) and maximal (**h**) fiber length in both male and female *Zdhhc7* KO vs. WT mice. Bars represent group means (± SEM) and asterisks depict the adjusted level of significance after Bonferroni correction for multiple testing (*T*: trend significance ($0.05<p<0.1$); *$p<0.05$; **$p<0.01$). Sample sizes of female KO–WT littermates were $n=4$, sample sizes of male KO–WT littermates $n=3$

(Scholz et al. 2015). Furthermore, Fish et al. (2018) correlated increased FA with prolonged EPM open arm time and suggested a relation with prenatal alcohol exposure-induced behavioral disinhibition. In the present study, DTI analyses revealed higher hippocampal minimum FA values in female *Zdhhc7* mutants resembling male minimum FA values (Fig. 5b). In addition, we observed prolonged open arm times indicating reduced anxiety-like behavior of female *Zdhhc7* mutants in the EPM (Fig. 2f). Together with their increased locomotion in all tests, this might point to a *Zdhhc7*-deficiency-induced behavioral disinhibition. Such behavioral disinhibition in favor of increased exploration was already described by others (Crawley 2007; Fish et al. 2018; Wilcoxon et al. 2007). All these changes could be caused by pronounced alterations in hippocampal network formation, structures, and connectivity in females, reflected by increased FA values and resulting in behavioral and functional adjustments.

Concluding remark

Overall, our newly generated mouse model demonstrated for the first time that constitutive inactivation of *Zdhhc7* causes alterations in brain structure/connectivity, function, and behavior of mice. These alterations were identified on a system level similarly affecting male and female brain structure and function. In contrast, other alterations differentially affected brain subregional microstructures, functions, and resulting behaviors in a predominantly sex-specific manner. Therefore, investigation of *Zdhhc7* mutants may provide additional knowledge with respect to the impact of ZDHHC7 on resulting sex differences. *Zdhhc7* deficiency might thus represent a promising model for further investigation of sex-specific alterations in the brain. Since hippocampus and mPFC are important parts of the cortico-limbic system related to anxiety, stress, and stress-induced mental disorders, it is conceivable that *Zdhhc7*-deficiency-mediated alteration might be even more accentuated under acute or chronic stress. In closing, *Zdhhc7*-deficient mice might provide a promising animal model for in-depth investigation of potentially underlying sex-specifically altered mechanisms, in particular with respect to humans and stress-related mental disorders.

Acknowledgements The authors thank Kathrin Schwarte from the Department of Psychiatry and Psychotherapy and Florian Breuer from the Department of Clinical Radiology, both University of Münster, Germany, for their excellent technical help and Stephanie Klco-Brosius for editorial advice. The work was supported by the Otto Creutzfeldt Center for Cognitive and Behavioral Neuroscience of the University of Münster, the Interdisciplinary Centre for Clinical Research (IZKF) of the University of Münster Medical School (Zha3-005-14 and core unit PIX), and by the Deutsche Forschungsgemeinschaft (ZH 34/3-1 to W.Z.).

Funding This study was funded by the Interdisciplinary Centre for Clinical Research (IZKF) of the University of Münster Medical School (Zha3-005-14 and core unit PIX) and by the Deutsche Forschungsgemeinschaft (ZH 34/3-1 to W.Z.). It was further supported by the Otto Creutzfeldt Center for Cognitive and Behavioral Neuroscience of the University of Münster.

Compliance with ethical standards

Conflict of interest The authors declare that they have no conflict of interest. No current external funding sources for this study had any role in study design, data collection and analysis, decision to publish, or preparation of the manuscript. Furthermore, the authors do not have any competing interests.

Research involving human and/or animal participants The presented work was in accordance with all current regulations covering animal experimentation in Germany and the EU (European Communities Council Directive 2010/63/EU). All experiments were approved by the local authority and the "Animal Welfare Officer" of the University of Münster.

Informed consent Informed consent was obtained from all authors included in the study.

References

Agarwal A, Zhang M, Trembak-Duff I, Unterbarnscheidt T, Radyushkin K, Dibaj P et al (2014) Dysregulated expression of neuregulin-1 by cortical pyramidal neurons disrupts synaptic plasticity. Cell Rep 8:1130–1145

Ambrée O, Klassen I, Forster I, Arolt V, Scheu S, Alferink J (2016) Reduced locomotor activity and exploratory behavior in CC chemokine receptor 4 deficient mice. Behav Brain Res 314:87–95

Anacker C, Scholz J, O'Donnell KJ, Allemang-Grand R, Diorio J, Bagot RC et al (2016) Neuroanatomic differences associated with stress susceptibility and resilience. Biol Psychiatry 79:840–849

Antinone SE, Ghadge GD, Lam TT, Wang L, Roos RP, Green WN (2013) Palmitoylation of superoxide dismutase 1 (SOD1) is increased for familial amyotrophic lateral sclerosis-linked SOD1 mutants. J Biol Chem 288:21606–21617

Baker KE, Parker R (2004) Nonsense-mediated mRNA decay: terminating erroneous gene expression. Curr Opin Cell Biol 16:293–299

Balthazart J, Ball GF (2006) Is brain estradiol a hormone or a neurotransmitter? Trends Neurosci 29:241–249

Bandler R, Keay KA, Floyd N, Price J (2000) Central circuits mediating patterned autonomic activity during active vs. passive emotional coping. Brain Res Bull 53:95–104

Baudry M, Bi X, Aguirre C (2013) Progesterone-estrogen interactions in synaptic plasticity and neuroprotection. Neuroscience 239:280–294

Boulware MI, Mermelstein PG (2009) Membrane estrogen receptors activate metabotropic glutamate receptors to influence nervous system physiology. Steroids 74:608–613

Boulware MI, Weick JP, Becklund BR, Kuo SP, Groth RD, Mermelstein PG (2005) Estradiol activates group I and II metabotropic glutamate receptor signaling, leading to opposing influences on cAMP response element-binding protein. J Neurosci 25:5066–5078

Brinton RD, Thompson RF, Foy MR, Baudry M, Wang J, Finch CE et al (2008) Progesterone receptors: form and function in brain. Front Neuroendocrinol 29:313–339

Butland SL, Sanders SS, Schmidt ME, Riechers SP, Lin DT, Martin DD et al (2014) The palmitoyl acyltransferase HIP14 shares a high proportion of interactors with huntingtin: implications for a role in the pathogenesis of Huntington's disease. Hum Mol Genet 23:4142–4160

Crawley JN (2007) What's wrong with my mouse? Behavioral phenotyping of transgenic and knockout mice, 2nd edn. Wiley, New York

Cryan JF, Kaupmann K (2005) Don't worry 'B'happy!: a role for GABAB receptors in anxiety and depression. Trends Pharmacol Sci 26:36–43

Damasio AR, Grabowski TJ, Bechara A, Damasio H, Ponto LL, Parvizi J et al (2000) Subcortical and cortical brain activity during the feeling of self-generated emotions. Nat Neurosci 3:1049–1056

Doyère V, Burette F, Negro CR, Laroche S (1993) Long-term potentiation of hippocampal afferents and efferents to prefrontal cortex: implications for associative learning. Neuropsychol 31:1031–1053

El-Husseini Ael-D, Bredt DS (2002) Protein palmitoylation: a regulator of neuronal development and function. Nat Rev Neurosci 3:791–802

Fernandez Marron, de Velasco E, Hearing M, Xia Z, Victoria NC, Luján R, Wickman K (2015) Sex differences in GABA(B)R-GIRK signaling in layer 5/6 pyramidal neurons of the mouse prelimbic cortex. Neuropharmacology 95:353–360

Fish EW, Wieczorek LA, Rumple A, Suttie M, Moy SS, Hammond P et al (2018) The enduring impact of neurulation stage alcohol exposure: a combined behavioral and structural neuroimaging study in adult male and female C57BL/6 J mice. Behav Brain Res 338:173–184

Franklin KBJ, Chudasama Y (2012) Chapter 30 - Prefrontal Cortex. In: Watson C, Paxinos G, Puelles L (eds) The Mouse Nervous System. Academic Press, San Diego, pp 727–735

Fukata Y, Fukata M (2010) Protein palmitoylation in neuronal development and synaptic plasticity. Nat Rev Neurosci 11:161–175

Galvin C, Ninan I (2014) Regulation of the mouse medial prefrontal cortical synapses by endogenous estradiol. Neuropsychopharmacology 39:2086–2094

Hammelrath L, Škokić S, Khmelinskii A, Hess A, van der Knaap N, Staring M et al (2016) Morphological maturation of the mouse brain: an in vivo MRI and histology investigation. Neuroimage 125:144–152

Hart SA, Snyder MA, Smejkalova T, Woolley CS (2007) Estrogen mobilizes a subset of estrogen receptor-alpha-immunoreactive vesicles in inhibitory presynaptic boutons in hippocampal CA1. J Neurosci 27:2102–2111

Hughes RN (2004) The value of spontaneous alternation behavior (SAB) as a test of retention in pharmacological investigations of memory. Neurosci Biobehav Rev 28:497–505

Jay TM, Burette F, Laroche S (1996) Plasticity of the hippocampal-prefrontal cortex synapses. J Physiol Paris 90:361–366

Jonas P, Bischofberger J, Sandkühler J (1998) Corelease of two fast neurotransmistters at a central synapse. Science 281:419–424

Kilpatrick CL, Murakami S, Feng M, Wu X, Lal R, Chen G et al (2016) Dissociation of Golgi-associated DHHC-type Zinc Finger Protein (GODZ)- and Sertoli Cell Gene with a Zinc Finger Domain-β (SERZ-β)-mediated Palmitoylation by Loss of Function Analyses in Knock-out Mice. J Biol Chem 291:27371–27386

Korycka J, Łach A, Heger E, Bogusławska DM, Wolny M, Toporkiewicz M et al (2012) Human DHHC proteins: a spotlight on the hidden player of palmitoylation. Eur J Cell Biol 91:107–117

Kreher BW, Hennig J, Il'yasov KA (2006) DTI&FiberTools: a complete toolbox for dti calculation, fiber tracking and combined evaluation. In: proceeding of ISMRM 14th international scientific meeting seattle, USA

Lemonidis K, Werno MW, Greaves J, Diez-Ardanuy C, Sanchez-Perez MC, Salaun C et al (2015) The zDHHC family of *S*-acyltransferases. Biochem Soc Trans 43:217–221

Linder ME, Deschenes RJ (2007) Palmitoylation: policing protein stability and traffic. Nat Rev Mol Cell Biol 8:74–84

Lynch MA (2004) Long-term potentiation and memory. Physiol Rev 84:87–136

Mateo Z, Porter JT (2007) Group II metabotropic glutamate receptors inhibit glutamate release at thalamocortical synapses in the developing somatosensory cortex. Neuroscience 146:1062–1072

Medrihan L, Tantalaki E, Aramuni G, Sargsyan V, Dudanova I, Missler M et al (2008) Early defects of GABAergic synapses in the brain stem of a MeCP2 mouse model of Rett syndrome. J Neurophysiol 99:112–121

Meitzen J, Mermelstein PG (2011) Estrogen receptors stimulate brain region specific metabotropic glutamate receptors to rapidly initiate signal transduction pathways. J Chem Neuroanat 42:236–241

Meitzen J, Grove DD, Mermelstein PG (2012) The organizational and aromatization hypotheses apply to rapid, nonclassical hormone action: neonatal masculinization eliminates rapid estradiol action in female hippocampal neurons. Endocrinology 153:4616–4621

Meitzen J, Luoma JI, Boulware MI, Hedges VL, Peterson BM, Tuomela K et al (2013) Palmitoylation of estrogen receptors is essential for neuronal membrane signaling. Endocrinology 154:4293–4304

Meitzen J, Britson KA, Tuomela K, Mermelstein PG (2017) The expression of select genes necessary for membrane-associated estrogen receptor signaling differ by sex in adult rat hippocampus. Steroids 142:21–27

Mitchell DA, Hamel LD, Reddy KD, Farh L, Rettew LM, Sanchez PR et al (2014) Mutations in the X-linked intellectual disability gene, zDHHC9, alter autopalmitoylation activity by distinct mechanisms. J Biol Chem 289:18582–18592

Mori S, Crain BJ, Chacko VP, van Zijl PC (1999) Three-dimensional tracking of axonal projections in the brain by magnetic resonance imaging. Ann Neurol 45:265–269

Nabekura J, Katsurabayashi S, Kakazu Y, Shibata S, Matsubara A, Jinno S et al (2004) Developmental switch from GABA to Glycine release in single central synaptic terminals. Nat Neurosci 7:17–23

Naumenko VS, Ponimaskin E (2018) Palmitoylation as a Functional Regulator of Neurotransmitter Receptors. Neur Plast 2018:5701348
Oberlander JG, Woolley CS (2016) 17β-Estradiol acutely potentiates glutamatergic synaptic transmission in the hippocampus through distinct mechanisms in males and females. J Neurosci 36:2677–2690
Oh SW, Harris JA, Ng L, Winslow B, Cain N, Mihalas S et al (2014) A mesoscale connectome of the mouse brain. Nature 508:207–214
Ohno Y, Kihara A, Sano T, Igarashi Y (2006) Intracellular localization and tissue-specific distribution of human and yeast DHHC cysteine-rich domain-containing proteins. Biochim Biophys Acta 1761:474–483
Ooishi Y, Kawato S, Hojo Y, Hatanaka Y, Higo S, Murakami G et al (2012) Modulation of synaptic plasticity in the hippocampus by hippocampus-derived estrogen and androgen. J Steroid Biochem Mol Biol 131:37–51
Palanza P, Parmigiani S (2017) How does sex matter? Behavior, stress and animal models of neurobehavioral disorders. Neurosci Biobehav Rev 76:134–143
Paxinos G, Franklin KBJ (2013) Paxinos and Franklin's the mouse brain in stereotaxic coordinates, 4th edn. Academic Press, San Diego
Pedram A, Razandi M, Deschenes RJ, Levin ER (2012) DHHC-7 and -21 are palmitoylacyltransferases for sex steroid receptors. Mol Biol Cell 23:188–199
Pilc A, Chaki S, Nowak G, Witkin JM (2008) Mood disorders: regulation by metabotropic glutamate receptors. Biochem Pharmacol 75:997–1006
Ponimaskin E, Dityateva G, Ruonala MO, Fukata M, Fukata Y, Kobe F et al (2008) Fibroblast growth factor-regulated palmitoylation of the neural cell adhesion molecule determines neuronal morphogenesis. J Neurosci 28:8897–8907
Saffari R, Teng Z, Zhang M, Kravchenko M, Hohoff C, Ambrée O et al (2016) NPY^+-, but not PV^+-GABAergic neurons mediated long-range inhibition from infra- to prelimbic cortex. Transl Psychiatry 6:e736
Sakalem ME, Seidenbecher T, Zhang M, Saffari R, Kravchenko M, Wördemann S et al (2017) Environmental enrichment and physical exercise revert behavioral and electrophysiological impairments caused by reduced adult neurogenesis. Hippocampus 27:36–51
Scholz J, Niibori Y, Frankland PW, Lerch JP (2015) Rotarod training in mice is associated with changes in brain structure observable with multimodal MRI. Neuroimage 107:182–189
Seney ML, Sibille E (2014) Sex differences in mood disorders: perspectives from humans and rodent models. Biology Sex Differ 5:17
Shipston MJ (2011) Ion channel regulation by protein palmitoylation. J Biol Chem 286:8709–8716
Spampinato SF, Molinaro G, Merlo S, Iacovelli L, Caraci F, Battaglia G et al (2012) Estrogen receptors and type 1 metabotropic glutamate receptors are interdependent in protecting cortical neurons against β-amyloid toxicity. Mol Pharmacol 81:12–20
Steinke KV, Gorinski N, Wojciechowski D, Todorov V, Guseva D, Ponimaskin E et al (2015) Human CLC–K channels require palmitoylation of their accessory subunit barttin to be functional. J Biol Chem 290:17390–17400
Suzuki H, Barros RP, Sugiyama N, Krishnan V, Yaden BC, Kim HJ et al (2013) Involvement of estrogen receptor β in maintenance of serotonergic neurons of the dorsal raphe. Mol Psychiatry 18:674–680
Tonn Eisinger KR, Woolfrey KM, Swanson SP, Schnell SA, Meitzen J, Dell'Acqua M et al (2018) Palmitoylation of caveolin-1 is regulated by the same DHHC acyltransferases that modify steroid hormone receptors. J Biol Chem 293:15901–15911
Tripathi A, Schenker E, Spedding M, Jay TM (2016) The hippocampal to prefrontal cortex circuit in mice: a promising electrophysiological signature in models for psychiatric disorders. Brain Struct Funct 221:2385–2391
Uylings HB, Groenewegen HJ, Kolb B (2003) Do rats have a prefrontal cortex? Behav Brain Res 146:3–17
Wehr MC, Hinrichs W, Brzózka MM, Unterbarnscheidt T, Herholt A, Wintgens J et al (2017) Spironolactone is an antagonist of NRG1-ERBB4 signaling and schizophrenia-relevant endophenotypes in mice. EMBO Mol Med 9:1448–1462
Wilcoxon JS, Nadolski GJ, Samarut J, Chassande O, Redei EE (2007) Behavioral inhibition and impaired spatial learning and memory in hypothyroid mice lacking thyroid hormone receptor alpha. Behav Brain Res 177:109–116
Wójtowicz T, Lebida K, Mozrzymas JW (2008) 17beta-estradiol affects GABAergic transmission in developing hippocampus. Brain Res 1241:7–17
Wright RA, Johnson BG, Zhang C, Salhoff C, Kingston AE, Calligaro DO et al (2013) CNS distribution of metabotropic glutamate 2 and 3 receptors: transgenic mice and [3H] LY459477 autoradiography. Neuropharmacology 66:89–98
Wu MV, Tollkuhn J (2017) Estrogen receptor alpha is required in GABAergic, but not glutamatergic, neurons to masculinize behavior. Horm Behav 95:3–12
Zagni E, Simoni L, Colombo D (2016) Sex and gender differences in central nervous system-related disorders. Neurosci J 2016:2827090

Affiliations

Christa Hohoff[1] · Mingyue Zhang[1] · Oliver Ambrée[1,2] · Mykola Kravchenko[1] · Jens Buschert[1,3] · Nicole Kerkenberg[1,3] · Nataliya Gorinski[4] · Dalia Abdel Galil[4] · Christiane Schettler[1] · Kari Lavinia vom Werth[1] · Maximilian F.-J. Wewer[1] · Ilona Schneider[1,3] · Dominik Grotegerd[1] · Lydia Wachsmuth[5] · Cornelius Faber[5] · Boris V. Skryabin[6,7] · Juergen Brosius[7,8] · Evgeni Ponimaskin[4] · Weiqi Zhang[1]

[1] Department of Psychiatry and Psychotherapy, University of Münster, Albert-Schweitzer-Campus 1/A9, 48149 Munster, Germany

[2] Department of Behavioral Biology, University of Osnabrück, Osnabrück, Germany

[3] Otto Creutzfeldt Center for Cognitive and Behavioral Neuroscience, University of Münster, Munster, Germany

[4] Cellular Neurophysiology, Center of Physiology, Hannover Medical School, Hannover, Germany

[5] Department of Clinical Radiology, University of Münster, Munster, Germany

[6] Department of Medicine, Core Facility Transgenic Animal and Genetic Engineering Models (TRAM), University of Münster, Munster, Germany

[7] Institute of Experimental Pathology, ZMBE, University of Münster, Munster, Germany

[8] Institutes for Systems Genetics, West China Hospital, Sichuan University, Chengdu 610041, China